COMPUTATION OF FLOW AROUND A CIRCULAR CYLINDER UNDERGOING TWO-DEGREE-OF-FREEDOM FORCED MOTION AT LOW REYNOLDS NUMBER

László Baranyi[1]
Department of Fluid and Heat Engineering
University of Miskolc
Miskolc
Hungary
Email: arambl@uni-miskolc.hu

ABSTRACT

This study investigates flow around a circular cylinder in forced two-degree-of freedom motion at four different phase angles between the transverse and in-line cylinder motion, at a Reynolds number of 250. Time-mean and rms values of force coefficients and mechanical energy transfer are investigated against frequency ratio in the lock-in domain. Computations were carried out by an in-house finite difference code developed by the author. Results reveal that an increase in phase angle, by bending the figure-eight cylinder path downstream, can reduce drag. Mechanical energy transfer was mostly positive, meaning that energy is transferred from the fluid to the cylinder, leading to a potentially dangerous VIV situation. The change in the initial conditions resulted in hardly any changes in the results.

NOMENCLATURE

$a_{0x,y}$	the dimensionless x and y components of cylinder acceleration
$A_{x,y}$	amplitude of oscillation in x or y directions, respectively, non-dimensionalised by d
C_D	drag coefficient, $2F_D/(\rho U^2 d)$
C_L	lift coefficient, $2F_L/(\rho U^2 d)$
d	cylinder diameter (m)
E	mechanical energy transfer
f	oscillation frequency, non-dimensionalised by U/d
f_v	vortex shedding frequency, non-dimensionalised by U/d
F_D	drag per unit length of cylinder (N/m)
F_L	lift per unit length of cylinder (N/m)
R	radius, non-dimensionalised by d
Re	Reynolds number, Ud/ν
St	non-dimensional vortex shedding frequency, $f_v d/U$
t	time, non-dimensionalized by d/U
T	motion period, $1/f_y$
U	free stream velocity, velocity scale (m/s)
$v_{0x,y}$	the dimensionless x and y components of cylinder velocity
x,y	Cartesian coordinates, non-dimensionalised by d
θ	phase angle difference between transverse and in-line cylinder motion
ρ	fluid density

Subscripts

D	drag
fb	fixed body
L	lift
rms	root-mean-square value
v	vortex shedding
x, y	components in x and y directions
0	for cylinder motion; for stationary cylinder at same Re; for initial condition
1	on the cylinder surface
2	on the outer boundary of the physical domain

INTRODUCTION

The flow past a single circular cylinder has been studied as a prototype of bluff body flows theoretically, experimentally and numerically. Some examples of these in real life are silos or smokestacks in wind or underwater pipes in a current. When vortices are shed from the structure a periodic force is generated which might lead to the vibration of the structure especially if the damping is small. The motion resulting from this force usually has either one or two degrees of freedom. The most frequently investigated type of one-degree-of-freedom (1-DoF) cylinder motion is the transverse cylinder oscillation. Both experimental and numerical studies have dealt with pure transverse cylinder motion (e.g., Williamson and Roshko, 1988; Lu and Dalton, 1996; Blackburn and Henderson, 1999. Less often investigated is pure in-line cylinder motion (e.g., Cetiner and Rockwell, 2001; Al-Mdallal et al., 2007; Mureithi et al., 2010).

However, far fewer investigations have been carried out for combined, two-degree-of-freedom (2-DoF) cylinder motion. In reality, however, both motions are often present, leading to a Lissajous-type path. The vortex-

Address all correspondence to this author[1]

induced vibration (VIV) arising in such cases can lead to problems such as fatigue and damage of structures.

Kheirkhah and Yarusevych (2010) suggest that where the mass ratio (the ratio of the mass of the vibrating system to the mass of the displaced fluid) is high, as mainly occurs when a structure is oscillating in air, then the frequency of oscillation in in-line and in transverse directions are approximately equal to each other. This can lead to an elliptical path, such as that observed in tube bundles in heat exchangers (Blevins, 1990). Studies by Didier and Borges (2007), Baranyi (2008) and Kheirkhah and Yarusevych (2010), among others, look at elliptical cylinder motion. The occurrence of vortex switches at certain amplitude values was noted (Baranyi, 2008).

A more typical Lissajous-type path, on the other hand, occurs with a low mass ratio, typically found when a cylinder is moving in liquid: cables and pipes submersed in flowing water may undergo fatigue or damage due to this kind of motion. In this case the frequency of the cylinder motion in in-line direction is approximately twice its frequency in transverse direction, as for example found by Jeon and Gharib (2001), Jauvtis and Williamson (2004), and Sanchis et al. (2008). The phase angle difference between in-line and transverse motion Θ results in different cylinder paths (Jeon and Gharib, 2001). One typical Lissajous curve is a figure-eight-shaped path, while a path in the shape of an arc, or C-shape, has also been observed in the experimental study for an elastically supported cylinder of Sanchis et al. (2008) in the Reynolds number domain of Re=(1.3 to 1.9)x10^4 and in the numerical work of Prasanth and Mittal (2009).

Figure-eight paths have been studied to some extent in numerical investigations with forced cylinder motion (e.g., Baranyi, 2011; Peppa et al., 2010). Both studies looked at the influence of the direction of motion along the figure-eight path; i.e., when the path is traced in a clockwise direction in the upper half or lobe of the figure (and naturally anticlockwise in the lower lobe), or vice versa. It was found that the orientation influenced the mechanical energy transfer: anticlockwise motion in the upper lobe (acw) resulted in positive energy transfer, meaning that the fluid tends to amplify the cylinder oscillation, which can easily lead to VIV. Force coefficients were also affected, with higher drag values for acw. Sanchis et al. (2008) found acw orientation in their free vibration study.

In their experimental study of flow around a forced 2-DoF cylinder motion, Jeon and Gharib (2001) investigated regular figure-eight paths and figure-eight patterns with the lobes bent slightly downstream. They state that the phase angle differences found ranged between Θ =0° and -45°. Similar distorted figure-eight paths were also found in Sanchis et al. (2008).

Based on the results of the above-mentioned experimental studies, a numerical simulation can be designed in order to investigate the effect of phase angle difference on the flow past a cylinder in 2-DoF figure-eight motion. Mechanical oscillation is used to simulate flow around the cylinder as a preliminary study, without carrying out a full fluid-structure interaction (FSI) study. While it is true that a direct relationship between results of investigations of free and of forced vibration is difficult to ascertain (e.g., Williamson, 2004), this is a first step towards considering FSI, with special attention to the energy transfer between the cylinder and fluid.

Low-Reynolds number simulation is sometimes criticised for being irrelevant to real-life cases, which almost always involve higher Reynolds (Re) numbers. However, as Newman and Karniadakis (1995) argue, since many phenomena in flow-induced vibrations are only weakly dependent on Re, they can be fairly accurately simulated even at relatively low Re.

In this numerical study a circular cylinder is placed in a uniform flow at Reynolds number Re=250 and mechanically oscillated in two directions, yielding various figure-eight paths (all anticlockwise in the upper lobe) for four phase angle differences. Mechanical energy transfer and the time-mean and root-mean-square (rms) values of force coefficients are investigated.

COMPUTATIONAL METHOD

A non-inertial system fixed to the accelerating cylinder is used to compute 2D low-Reynolds number unsteady flow around a circular cylinder placed in a uniform stream. The governing equations are the non-dimensional Navier-Stokes equations for incompressible constant-property Newtonian fluid in a non-inertial system fixed to the accelerating cylinder, the equation of continuity and the Poisson equation for pressure.

On the cylinder surface, no-slip boundary condition is used for the velocity and a Neumann type boundary condition is used for the pressure. At the far region, potential flow is assumed. Computational results show that this approximation results in some inaccuracies near the outer boundary only, and in practice it has no influence on the results of the near-wake flow and forces acting on the cylinder.

Boundary-fitted coordinates are used to impose the boundary conditions accurately. The physical domain bounded by two concentric circles with radii R_1 and R_2 is mapped into a rectangular computational domain with equidistant spacing in both directions (see Fig. 1). In the physical domain logarithmically spaced radial cells are used, providing a fine grid scale near the cylinder wall and a coarse grid in the far field. The transformed governing equations and boundary conditions are solved by finite difference method. Space derivatives are approximated by fourth order central differences, except for the convective terms for which a third order modified upwind scheme is used. The Poisson equation for pressure is solved by the successive over-relaxation (SOR) method. The Navier-Stokes equations are integrated explicitly and continuity is satisfied at every time step. For further details see Baranyi (2003; 2008).

The 2D code developed by the author has been extensively tested against experimental and computational

results with good agreement being found, (Baranyi, 2008). A systematic comparison with results from the commercial software package Ansys Fluent also yielded very good agreement (Baranyi et al., 2011).

In this study the dimensionless time step is 0.0005, the number of grid points is 481x451, and a relatively large physical domain of R_2/R_1=360 has been chosen to enhance accuracy.

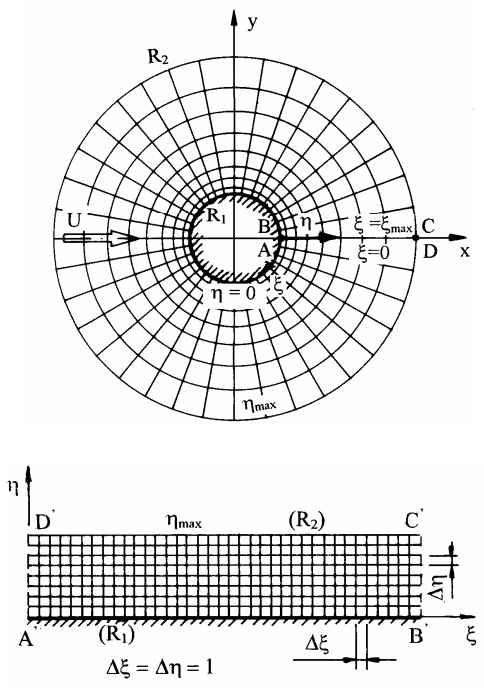

Figure 1. Physical and computational domains

This study investigates the behaviour of flow past a cylinder placed in a uniform stream with its axis perpendicular to the main flow. The cylinder is oscillated mechanically in both in-line and transverse directions in relation to the uniform stream. The dimensionless displacement of forced cylinder motion given in the experimental study of Jeon and Gharib (2001) is adopted here, defined as

$$x_0=A_x \sin(4\pi f_y (t-t_0)+\Theta); \quad y_0= A_y \sin(2\pi f_y (t-t_0)), \quad (1)$$

where A_x and A_y are the dimensionless oscillation amplitudes and f_y is the frequency of oscillation in transverse direction. Here t and t_0 are non-dimensional time, with t_0 being the initial condition, and Θ is the phase angle difference between the two oscillations. The second time derivatives of x_0 and y_0 give the accelerations that occur in the Navier-Stokes equations.

Jeon and Gharib (2001) suggest that the value of phase angle Θ tends to drift for free-vibration cases, but is usually in the range of 0 to – 45°. Different phase angle values result in different cylinder paths. Based on the suggestion of Jeon and Gharib (2001) Θ =0°, -15°, -30°, and -45° are investigated here. As shown in Fig. 2, Θ =0° gives a symmetric figure-8-path; whereas at Θ = -45° the path is a figure-8 pattern with the lobes bent downstream. The dimensionless oscillation amplitudes in this study are fixed at A_x=0.1 and A_y=0.4 throughout the study, ensuring slender cylinder paths. The Reynolds number is fixed at Re=250. The independent variable for the investigation is the frequency ratio of f_y/St_0 ranging from around 0.7 to 1.1 (in the vicinity of the natural vortex shedding frequency f_y/St_0=1), but limited to within the lock-in domain. Here St_0 is the dimensionless vortex shedding frequency for a stationary cylinder at the same Reynolds number. For Re=250 the value St_0=0.20355 was used (from Posdziech and Grundmann, 2007).

Since initial condition was earlier found to influence the number and/or location of jumps in the TM and rms values of force coefficients for a cylinder in 2-DoF motion (Baranyi, 2008), computations were carried out for three different initial conditions (t_0=0, 0.5, 1.0) for Θ = -15°. For the other Θ values the initial condition was t_0=0.

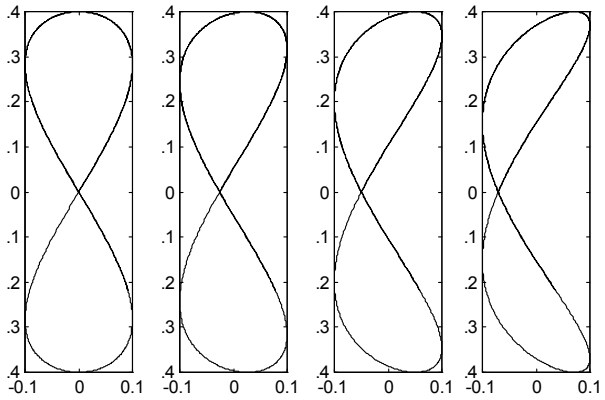

Θ=0° **Θ=-15°** **Θ=-30°** **Θ=-45°**

Figure 2. Cylinder paths for different phase angles Θ

The time-history of force coefficients (lift, drag, base pressure and torque), pressure and velocity field are computed. From these data, time-mean (TM) and root-mean-square (rms) values of force coefficients, streamlines, and vorticity contours can be obtained. Where jumps are found when force coefficients are plotted against frequency ratio, pre- and post-jump analysis is carried out by investigating limit cycle curves, time history curves, FFT spectra and vorticity contours.

Throughout this paper the lift and drag coefficients used do not contain the inertial forces originated from the non-inertial system fixed to the accelerating cylinder, except for the determination of the mechanical energy transfer E. Coefficients obtained by removing the inertial forces are often termed 'fixed body' coefficients (see Lu and Dalton, 1996). The relationship between the two sets of coefficients can be written as

$$C_D=C_{D\,fb}+\pi\, a_{0x}/2, \quad C_L=C_{L\,fb}+\pi\, a_{0y}/2 \qquad (2)$$

where a_{0x} and a_{0y} are the cylinder acceleration components and subscript 'fb' refers to the fixed body (understood in an inertial system fixed to the stationary cylinder), Baranyi (2005). Since the inertial terms are periodic functions, their TM values vanish, resulting in identical TM values for lift and drag in the inertial and non-inertial systems. Naturally the rms values of C_L and C_D will be somewhat different in the two systems.

Investigation was restricted to lock-in cases. Lock-in, or the synchronization between vortex shedding and cylinder motion, produces a periodic solution for each of the force coefficients. In this paper, we consider lock-in to be when the vortex shedding frequency is identical to f_y, the frequency of transverse cylinder oscillation.

The non-dimensional mechanical energy transfer originally introduced by Blackburn and Henderson (1999) for transversely oscillated cylinder was extended for a general 2-DoF motion of the cylinder by Baranyi (2008):

$$E = \frac{2}{\rho U^2 d^2} \int_0^T \mathbf{F} \cdot \mathbf{v}_0 \, \mathrm{d}t = \int_0^T \left(C_D \, v_{0x} + C_L \, v_{0y} \right) \mathrm{d}t \,, \qquad (3)$$

where $T=1/f_y$ is the motion period chosen, v_{0x} and v_{0y} are the x and y components of cylinder velocity. Note that Eq. (3) is valid for 1-DoF cylinder motion as well.

RESULTS

In this study, computations are carried out for the flow past a cylinder following a distorted figure-8-path at Re=250 against frequency ratio f_y/St_0 within the lock-in domain. Mechanical energy transfer E between the cylinder and the fluid, time-mean (TM) and rms values of lift C_L, drag C_D, base pressure and torque coefficients are investigated, but for the sake of simplicity only C_L, C_D and E values will be shown in the paper. Sudden jumps between state curves were found in some cases; these indicate a sudden change in the vortex structure (Baranyi, 2008). Values just before and just after a jump (vortex switch) are presented in a pre- and post-jump analysis.

Time-mean and rms values

At all four phase angle values investigated, the TM of lift and torque coefficients was zero throughout the locked-in frequency domain (not shown here). This has also been found for all transversely oscillated cases investigated by the author. The rms of fixed-body lift, shown in Fig. 3, generally increases with frequency ratio for all Θ values. A tendency that can be observed in Fig. 3 above the frequency ratio of 0.84 is that the absolute value of Θ increases with f_y/St_0. Some jumps can be seen in the curves. The curve belonging to Θ= -45° is not even continuous, because – in accordance with the findings of Gharib (1999) – for Θ = - 45° a not-locked-in domain exists that is bounded by two lock-in domains.

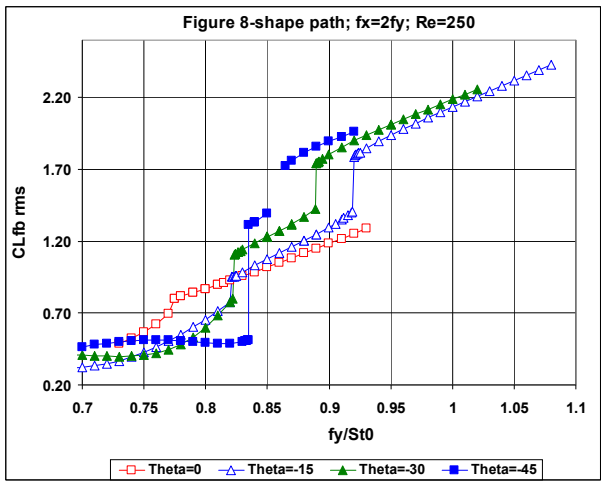

Figure 3. Rms of lift versus frequency ratio for phase angles Θ=0°, -15°, -30° and -45°

The TM of drag versus frequency ratio for the four phase angle values is shown in Fig. 4 in the lock-in domain. It can be seen that the TM of drag decreases with larger absolute values of the phase angle over most of the lock-in frequency ratio domain for the given parameters. Clear changes in behaviour are seen between Θ=0° and the other Θ values; as the path is bent downstream, the drag is drastically reduced, while sudden jumps in the curve appear, indicating an abrupt switch in vortex structure (see e.g. Baranyi, 2008).

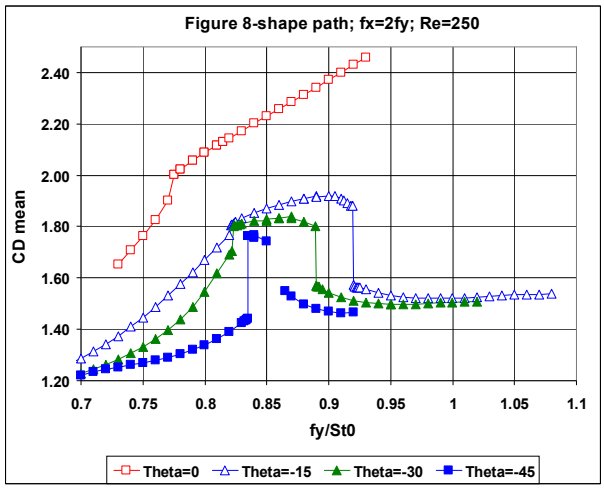

Figure 4. Time-mean of drag versus frequency ratio for phase angles Θ=0°, -15°, -30° and -45°

The rms of fixed body drag against frequency ratio can be seen in Fig. 5. It seems that the values for Θ=0° are much higher than C_{Dfbrms} values belonging to other Θ values. As can be seen in the figure, the curves belonging to Θ= -15°, -30° and -45° are grouped together. As no substantial jump can be observed in the figure, it seems that vortex switches do no not have much effect on C_{Dfbrms} values, probably due to symmetry.

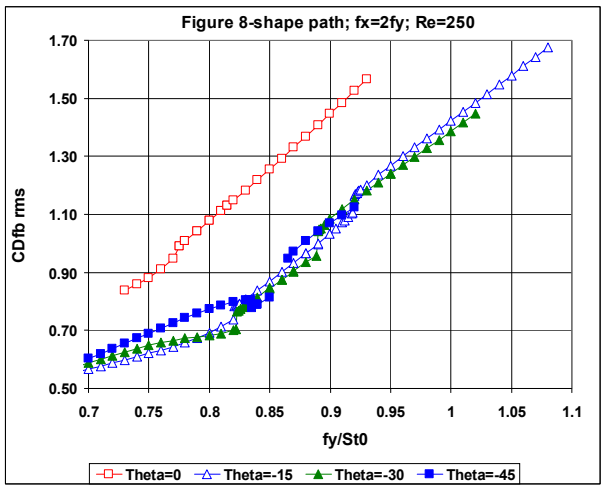

Figure 5: Rms of drag versus frequency ratio for phase angles Θ=0°, -15°, -30° and -45°

Mechanical energy transfer

Figure 6 shows the mechanical energy transfer E between the fluid and cylinder. For Θ=0° and at the amplitudes of A_x and A_y investigated, E remained positive throughout the lock-in domain, and practically constant from 0.77 to 0.93. For the other three values, although the largest part of the lock-in domain exhibits positive mechanical energy transfer values, there are some sub-domains where E is negative. Positive E means that energy is introduced into the cylinder and in the case of free vibration, this could well lead to VIV. It can also be seen in the figure that E decreases with larger phase angle differences.

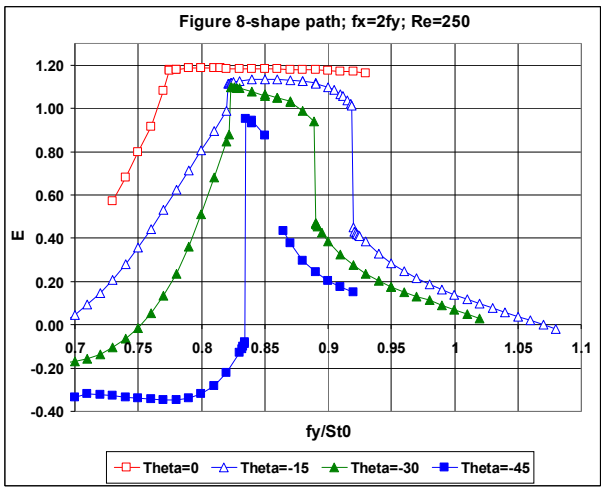

Figure 6. Mechanical energy transfer vs. frequency ratio for phase angles Θ=0°, -15°, -30° and -45°

Effect of initial condition

As is well known, a main feature of non-linear systems is that their solutions can be very sensitive to the initial condition. A very small change in the initial conditions can result in a drastic change in the solution. To check whether this is the case here computations for Θ= -15°, first carried out at t_0=0, were repeated for t_0=0.5 and 1.0 (see Eq. (1)). In contrary to previous findings in Baranyi (2008) for an elliptical path, where the location of jumps was affected strongly by the initial condition, here the solutions basically were independent of the initial conditions: the three curves collapse into one, as can be seen in Figs. 7 and 8. Note that the curve for the TM of drag in Fig. 7 is the same as that denoted by blue empty triangles in Fig. 4, while the mechanical energy transfer curve shown in Fig. 8 is seen also in Fig. 6. Curves for all other variables also coincided for the three different t_0 values. For these parameters, it can thus be stated that the initial condition has essentially no effect on the flow.

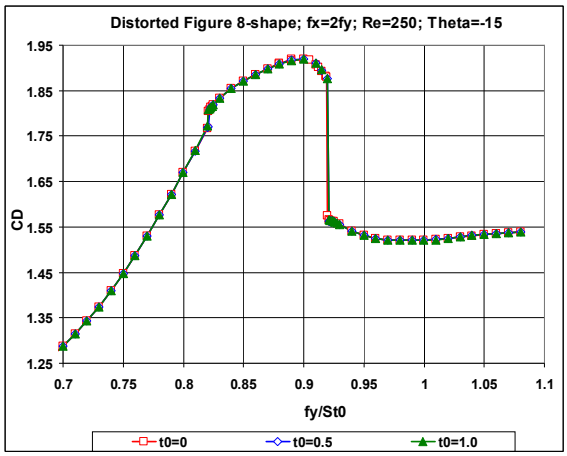

Figure 7. Time-mean of drag vs. frequency ratio for phase angle Θ=-15° and t_0=0, 0.5, 1.0

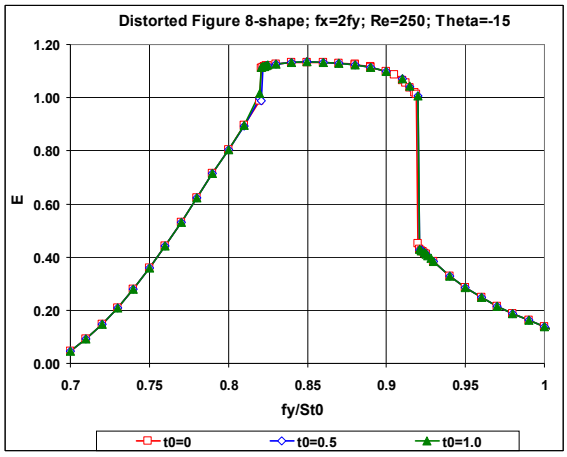

Figure 8. Mechanical energy transfer vs. frequency ratio for phase angle Θ=-15° and t_0=0, 0.5, 1.0

Pre- and post-jump analysis

As can be seen in most of the figures, sudden jumps in the curves can be seen at some frequency ratio values, which can probably be attributed to vortex switches. The vicinity of a jump is investigated by different means, such as the time history of fixed body lift, limit cycle curves and vorticity contours before and after a jump. Due to lack

of space pre- and post-jump results will be shown only for the single case of Θ= -45°, with frequency ratios on the two sides of the jump of $(f_y/St_0)_1$=0.8345 and $(f_y/St_0)_2$=0.835.

The time histories of the periodic part of the fixed body lift for the two frequency ratios are shown against the dimensionless time t in Fig. 9. Pre-jump curves are denoted by red lines and post-jump curves by blue lines in Figs. 9 and 10. As can be seen in the figure, despite the tiny difference in the frequency ratios, the two time-history curves are substantially different.

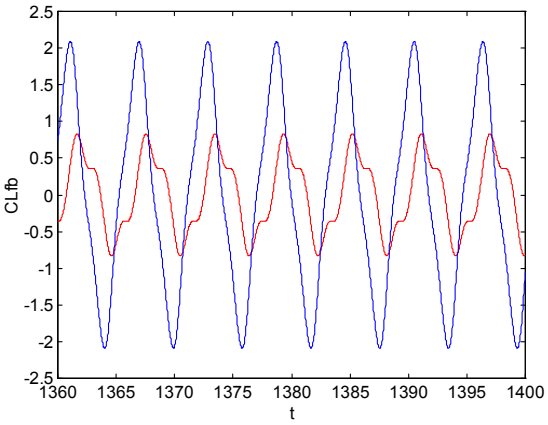

Figure 9. Time history of fixed body lift (red line: f_y/St_0=0.8345; blue line: f_y/St_0=0.835)

The limit cycle curves (C_{Dfb},C_{Lfb}) can be seen in Fig. 10 for the pre-jump and post-jump frequency ratios. The very small difference in frequency ratio results in a drastic change in the shape of the two limit cycle curves Interestingly, both curves have reflection symmetry. This is true for the drag-lift limit cycle curves of every computational point with a periodic solution. This symmetry originates from the fact that the drag is the same for both positive and negative y_0 displacement values.

When C_{Lfb} and its time derivative $\dot{C}_{Lfb}$ are plotted only at the multiples of the motion period T a Poincaré map is obtained, which can be interpreted as a discrete dynamical system. Here, we investigate the limit cycle curves (C_{Lfb},$\dot{C}_{Lfb}$) containing all the points in the phase plane as a continuous function of time, for pre-jump (Fig. 11) and post-jump (Fig. 12) frequency ratios. Again, noticeable differences occur. The curve in Fig. 11 exhibits two cusps, and is much smaller than the post-jump curve in Fig. 12, which is a relatively smooth curve.

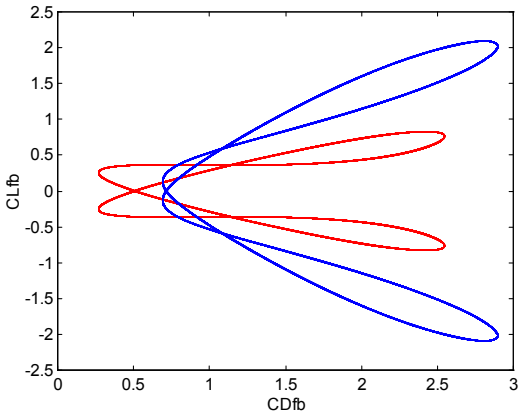

Figure 10. Limit cycle (C_{Dfb},C_{Lfb}) for Θ=-45°; f_y/St_0=0.8345 (red) and 0.835 (blue)

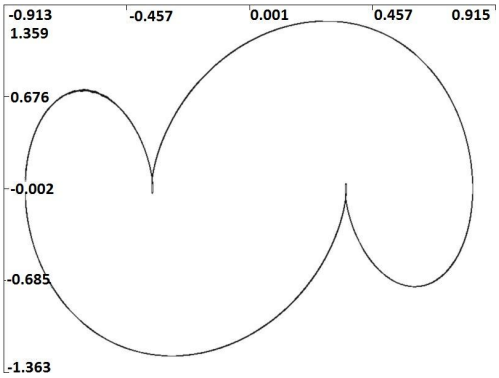

Figure 11. Limit cycle (C_{Lfb},$\dot{C}_{Lfb}$) for Θ=-45°; f_y/St_0=0.8345 (pre-jump)

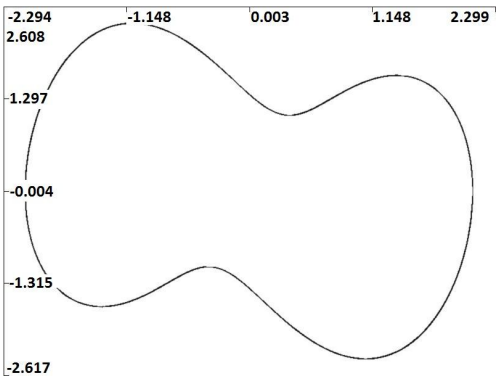

Figure 12. Limit cycle (C_{Lfb},$\dot{C}_{Lfb}$) for Θ=-45°; f_y/St_0=0.835 (post-jump)

Vorticity contours are presented for pre-jump (Fig. 13) and post-jump (Fig. 14) frequency ratio values. The blue lines indicate negative vorticity values (clockwise rotation), and the red lines show positive values (anticlockwise rotation). The contours belong to the same

cylinder position, at t=240T, by which time the solution is fully periodic.

With pure in-line oscillation mirror image switches have been observed, so the pattern remains the same type (in the cases investigated, one pair of vortices is shed in one cycle) (Baranyi et al., 2010). This was probably caused by symmetry-breaking bifurcation (see e.g. Crawford and Knobloch, 1991). For tranverse cylinder oscillation no switches were found, and the 2S pattern (a single vortex shed from each side of the cylinder within a single cycle; see Williamson and Roshko, 1988) appears to be typical around Re=250 (Baranyi et al. 2011). With elliptical motion, the solution flips but appears to move further from the mirror image solution as the transverse component increases (Baranyi, 2008). In this case, the flow patterns do not seem to flip in the vicinity of the cylinder, but a striking difference in flow structure can be seen. Figure 13 shows what appears to be 2P shedding (a pair shed from each side of the cylinder in one cycle), while the post-jump pattern seems to be 2S, rather similar to the Kármán vortex street but with a broader wake.

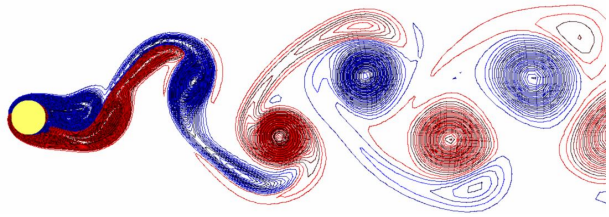

Figure 13. Vorticity contours at t=240T for Θ=-45°; f_y/St_0=0.8345 (pre-jump)

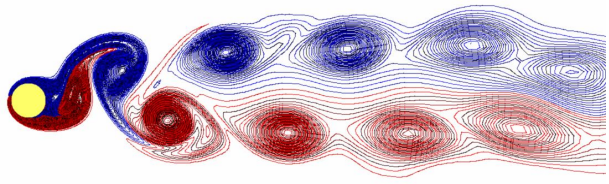

Figure 14. Vorticity contours at t=240T for Θ=-45°; f_y/St_0=0.835 (post-jump)

CONCLUSIONS

Low-Reynolds number flow around a circular cylinder in two-degree-of-freedom forced motion is investigated numerically at the Reynolds number of 250. Computations were carried out at four different phase angles of Θ=0°, -15°, -30° and -45°, ranging from a symmetrical to a distorted figure-eight shape, with an anticlockwise direction of orientation in the upper lobe.

The numerical investigation revealed that larger phase angle differences can reduce drag by bending the figure-eight cylinder path further downstream.

Mechanical energy transfer also decreases with increasing phase angle difference, but remains mostly in the positive domain, meaning that energy is transferred from the fluid to the cylinder, thus leading to a potentially dangerous VIV situation.

At all four phase angle values investigated, the time-mean of lift and torque coefficients was zero throughout the locked-in frequency domain.

The initial condition had scarcely any effect on the solution for Θ= -15°.

Where jumps in time-mean or rms values representing vortex switches were identified, pre- and post-jump analysis was carried out, revealing different time-history and limit cycle curves, vorticity contours and even different vortex shedding patterns.

As this study investigated only an anticlockwise direction of orbit, further investigation could include repeating computations for the clockwise case or at other Reynolds numbers or oscillation amplitude values.

ACKNOWLEDGMENTS

The support provided by the Hungarian Scientific Research Fund under contract No. OTKA K 76085 is gratefully acknowledged. The author thanks Mr. L. Daróczy for designing the flow visualization software used in Figs. 11-14. The work was carried out as part of the TÁMOP-4.2.1.B-10/2/KONV-2010-0001 project in the framework of the New Hungarian Development Plan. The realization of this project is supported by the European Union, co-financed by the European Social Fund.

REFERENCES

Al-Mdallal, Q.M., Lawrence, K.P. and Kocabiyik, S., 2007, "Forced streamwise oscillations of a circular cylinder: Locked-on modes and resulting fluid forces," *Journal of Fluids and Structures* **23**, 681-701.

Baranyi, L., 2003, "Computation of unsteady momentum and heat transfer from a fixed circular cylinder in laminar flow," *Journal of Computational and Applied Mechanics* **4**(1), 13-25.

Baranyi, L., 2005, "Lift and drag evaluation in translating and rotating non-inertial systems," *Journal of Fluids and Structures* **20**(1), 25-34.

Baranyi, L., 2008, "Numerical simulation of flow around an orbiting cylinder at different ellipticity values," *Journal of Fluids and Structures* **24**, 883-906.

Baranyi, L., Huynh, K. and Mureithi, N.W., 2010, "Dynamics of flow behind a cylinder oscillating in-line for low Reynolds numbers," Proc. *7th International Symposium on Fluid-Structure Interactions, Flow-Sound Interactions, and Flow-Induced Vibration and Noise,* (*within FEDSM2010-ICNMM2010 ASME Conference 2010*), Montreal, Québec, Canada, on CD ROM, pp. 1-10, Paper No. FEDSM-ICNMM2010-31183

Baranyi, L., 2011, "Low-Reynolds number flow around a cylinder following a figure-8 path -- effect of direction

of orbit," Proc. *IUTAM Symposium on Bluff Body Flows*, Kanpur, India, pp. 21-24.

Baranyi, L., Bolló, B. and Daróczy, L., 2011, "Simulation of low-Reynolds number flow around an oscillated cylinder using two computational methods," Proc. *ASME 2011 Pressure Vessels and Piping Division Conference PVP2011*, Baltimore, Maryland, USA, pp. 1-9, Paper No. PVP2011-57554

Blackburn, H.M. and Henderson, R.D., 1999, "A study of two-dimensional flow past an oscillating cylinder," *Journal of Fluid Mechanics* **385**, 255-286.

Blevins, R.D., 1990, *Flow-Induced Vibrations*. Van Nostrand Reinhold, New York.

Cetiner, O. and Rockwell, D., 2001, "Streamwise oscillation of a cylinder in a steady current. Part 1. Locked-on states of vortex formation and loading," *Journal of Fluid Mechanics* **427**, 1-28.

Crawford, J.D. and Knobloch, E., 1991, "Symmetry and symmetry-breaking bifurcations in fluid dynamics," *Annual Review of Fluid Mechanics* **23**, 341-387.

Didier, E. and Borges, A.R.J., 2007, "Numerical predictions of low Reynolds number flow over an oscillating circular cylinder," *Journal of Computational and Applied Mechanics* **8**(1), 39-55.

Gharib, M.R., 1999, "Vortex-induced vibration, absense of lock-in and fluid force deduction," *PhD dissertation*, GALCIT, California Institute of Technology, Pasadena, CA, U.S.A.

Jauvtis, N. and Williamson, C. H. K., 2004, "The effect of two degrees of freedom on vortex-induced vibration and at low mass and damping," *Journal of Fluid Mechanics* **509**, 23–62.

Jeon, D. and Gharib, M., 2001, "On circular cylinders undergoing two-degree-of-freedom forced motions," *Journal of Fluids and Structures* **15**, 533-541.

Kheirkhah, S. and Yarusevych, S., 2010, "Two-degree-of-freedom flow-induced vibrations of a circular cylinder with a high moment of inertia ratio," *Proc. ASME 2010 3rd Joint US-European Fluids Engineering Summer Meeting and 8th Int. Conference on Nanochannels, Microchannels, and Minichannels (FEDSM-ICNM2010)*, Montreal, Québec, Canada, on CD ROM, pp. 1-10, Paper No. FEDSM-ICNMM2010-30042

Lu, X.Y. and Dalton, C., 1996, "Calculation of the timing of vortex formation from an oscillating cylinder," *Journal of Fluids and Structures* **10**, 527-541.

Mureithi, N.W., Huynh, K., Rodriguez, M. and Pham, A., 2010, "A simple low order model of forced Karman wake," *International Journal of Mechanical Sciences* **52**(11), 1522-1534.

Newman, D.J., and Karniadakis, G.E., 1995, "Direct numerical simulation of flow over a flexible cable", Proc. *6th Int. Conference on Flow-Induced Vibration*, London, pp. 193-203 .

Peppa, S., Kaiktsis, L. and Triantafyllou, G.S., 2010, "The effect of in-line oscillation on the forces of a cylinder vibrating in a steady flow," Proc. *7th International Symposium on Fluid-Structure Interactions, Flow-Sound Interactions, and Flow-Induced Vibration and Noise,* (*within FEDSM2010-ICNMM2010 ASME Conference 2010*), Montreal, Québec, Canada, on CD ROM, pp. 1-8, Paper No. FEDSM-ICNMM2010-30054

Prasanth, T.K. and Mittal, S., 2009, "Flow-induced oscillation of two circular cylinders in tandem arrangement at low Re," *Journal of Fluids and Structures* **25**, 1029-1048.

Posdziech, O. and Grundmann, R., 2007, "A systematic approach to the numerical calculation of fundamental quantities of the two-dimensional flow over a circular cylinder," *Journal of Fluids and Structures* **23**, 479-499.

Sanchis, A., Sælevik, G., Grue, J., 2008, "Two-degree-of-freedom vortex-induced vibrations of a spring-mounted rigid cylinder with low mass ratio," *Journal of Fluids and Structures* **24**, 907-919.

Williamson, C.H.K. and Roshko, A., 1988, "Vortex formation in the wake of an oscillating cylinder," *Journal of Fluids and Structures* **2**, 355-381.

Williamson, C.H.K., 2004, "Vortex-induced vibrations," *Annual Review of Fluid Mechanics* **36**, 413-455.